

BIOCHEMISTRY

Exonuclease VII repairs quinolone-induced damage by resolving DNA gyrase cleavage complexes

Shar-yin N. Huang^{1*}, Stephanie A. Michaels¹, Brianna B. Mitchell¹, Nadim Majdalani², Arnaud Vanden Broeck³, Andres Canela⁴, Yuk-Ching Tse-Dinh⁵, Valerie Lamour³, Yves Pommier^{1*}

The widely used quinolone antibiotics act by trapping prokaryotic type IIA topoisomerases, resulting in irreversible topoisomerase cleavage complexes (TOPcc). Whereas the excision repair pathways of TOPcc in eukaryotes have been extensively studied, it is not known whether equivalent repair pathways for prokaryotic TOPcc exist. By combining genetic, biochemical, and molecular biology approaches, we demonstrate that exonuclease VII (ExoVII) excises quinolone-induced trapped DNA gyrase, an essential prokaryotic type IIA topoisomerase. We show that ExoVII repairs trapped type IIA TOPcc and that ExoVII displays tyrosyl nuclease activity for the tyrosyl-DNA linkage on the 5'-DNA overhangs corresponding to trapped type IIA TOPcc. ExoVII-deficient bacteria fail to remove trapped DNA gyrase, consistent with their hypersensitivity to quinolones. We also identify an ExoVII inhibitor that synergizes with the antimicrobial activity of quinolones, including in quinolone-resistant bacterial strains, further demonstrating the functional importance of ExoVII for the repair of type IIA TOPcc.

INTRODUCTION

Topoisomerases are the target of widely used anticancer drugs and antibiotics (1–5). Quinolone antibiotics, in particular, ciprofloxacin, are on the World Health Organization's List of Essential Medicines (6, 7). Collectively termed as topoisomerase poisons, these drugs bind to a transient pocket at the covalent enzyme-DNA interface during the catalytic cycles of topoisomerases as they cleave DNA backbone(s) to adjust DNA topology (1, 3, 8, 9). Trapping of topoisomerase-DNA cleavage complexes (TOPcc) is the initiating event in the killing of bacteria and cancer cells by antibacterial and anticancer topoisomerase poisons, respectively. Previous studies revealed that the repair of TOPcc in eukaryotes relies on their excision by the tyrosyl-DNA phosphodiesterase (TDP1 and TDP2) enzymes, which hydrolyze the covalent bond between the trapped topoisomerase catalytic tyrosine and the DNA end (10). Thus, eukaryotic TDP enzymes have become rational drug targets as their inactivation synergizes with anticancer topoisomerase poisons (10). Yet, despite the wide usage of quinolones, the repair pathways of prokaryotic TOPcc are much less understood than the repair of TOPcc in eukaryotes, and until now, no TDP activity has been identified in prokaryotes.

Escherichia coli strains deficient in DNA double-strand break repair or the RuvABC resolvosome machinery (involved in Holliday junction resolution) are hypersensitive to ciprofloxacin, as these pathways are likely required for rejoining the DNA ends after the excision of the TOPcc (11, 12). Intriguingly, loss of exonuclease VII (ExoVII), a nuclease capable of degrading single-stranded DNA in vitro but without well-defined biological functions (13), has been

associated with hypersensitivity to quinolones (11, 12, 14–16). This observation led us to examine whether ExoVII, a multimeric complex composed of a catalytic subunit, XseA (encoded by *xseA*), and multiple regulatory subunits, XseB (encoded by *xseB*), could act as a repair nuclease for trapped TOPcc in bacteria. In the current study, we combine genetic, biochemical, and molecular biology approaches to demonstrate that ExoVII repairs quinolone-induced DNA damage by excising trapped DNA gyrase. We also identify an ExoVII inhibitor that synergizes with the antimicrobial activity of ciprofloxacin and could potentially increase the efficacy of quinolones, particularly in the strains that have developed quinolone resistance.

RESULTS

ExoVII-deficient *E. coli* strains are hypersensitive to trapped type IIA topoisomerase

To understand the role of ExoVII in the repair of quinolone-induced DNA damage, we first confirmed that inactivation of ExoVII in *E. coli* leads to hypersensitivity to ciprofloxacin, which traps type IIA TOPcc (8). Compared to wild-type (WT) strains, deficiency in either subunit of ExoVII ($\Delta xseA$ or $\Delta xseB$) decreased the minimum inhibitory concentration (MIC) of ciprofloxacin by 60 to 70% (Fig. 1A and fig. S1, A and B). ExoVII-deficient strains are not hypersensitive to the non-quinolone topoisomerase catalytic inhibitor novobiocin (15), suggesting that ExoVII is specifically involved in repairing trapped DNA gyrase rather than damages stemming from the loss of DNA gyrase activity.

Bacterial strains in the clinical settings frequently develop quinolone resistance by acquiring mutations in the quinolone resistance-determining region that lead to reduced binding of quinolones to the type IIA topoisomerases (17–19). To determine whether inactivating ExoVII in quinolone-resistant strains can resensitize bacteria to quinolones, we genetically modified DNA gyrase, the primary target of quinolones among the two type IIA topoisomerases in *E. coli*. We introduced a leading recurrent mutation to the DNA gyrase GyrA subunit, *gyrA*-S83L (20), that leads to quinolone resistance. Because DNA gyrase is essential in *E. coli*, we first transformed the

¹Laboratory of Molecular Pharmacology, Developmental Therapeutics Branch, Center for Cancer Research, National Cancer Institute, NIH, Bethesda, MD 20892, USA.

²Laboratory of Molecular Biology, Center for Cancer Research, National Cancer Institute, NIH, Bethesda, MD 20892, USA. ³Integrated Structural Biology Department, IGBMC, UMR7104 CNRS, U1258 Inserm, University of Strasbourg, Illkirch 67404, France. ⁴The Hakubi Center for Advanced Research, Radiation Biology Center, Graduate School of Biostudies, Kyoto University, Yoshida-Konoe-cho, Sakyo-ku, Kyoto 606-8501, Japan. ⁵Department of Chemistry and Biochemistry, Biomolecular Sciences Institute, Florida International University, Miami, FL 33199, USA.

*Corresponding author. Email: shar-yin.huang@nih.gov (S.-y.N.H.); pommier@nih.gov (Y.P.)

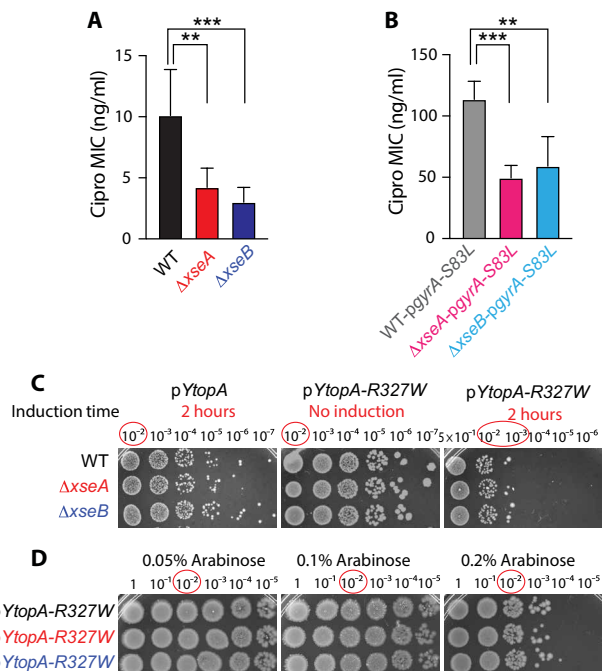


Fig. 1. Loss of ExoVII sensitizes *E. coli* strains with both the WT and quinolone-resistant backgrounds to ciprofloxacin, which traps type IIA topoisomerases.

By contrast, loss of ExoVII does not sensitize *E. coli* to trapped type IA topoisomerase (A). Average MIC values for ciprofloxacin (Cipro) in WT strain or strains deficient in either subunit of ExoVII ($\Delta xseA$ and $\Delta xseB$) ($n \geq 4$). Statistical significance was calculated using two-tailed Student's *t* test in GraphPad Prism. $**P < 0.01$. $***P < 0.001$. (B) Same as in (A), except that the *E. coli* strains express the quinolone-resistant mutation in the catalytic subunit of DNA gyrase, *GyrA-S83L* (*pgyrA-S83L*) (17–19), followed by inactivation of the genomic copy of *gyrA* (fig. S1C). As expected, the mutation *gyrA-S83L* led to resistance to ciprofloxacin, reflected by a 10-fold increase in ciprofloxacin MIC (compare Fig. 1, A and B). Inactivating either subunit of ExoVII in the *gyrA-S83L* strain resensitized the bacteria to quinolones by ~2-fold (Fig. 1B and fig. S1D) (12, 21), demonstrating the functional importance of ExoVII in the quinolone-resistant bacteria strains. (C) Transformants with *pY. pestis topA* (*pYtopA*, encoding YTop1) or *pY. pestis topA-R327W* (*pYtopA-R327W*, encoding YTop1-R327W) were established in either the WT, $\Delta xseA$, or $\Delta xseB$ strains. Left panel shows the spotted growth of serial dilutions of *pYtopA* transformants after induction with 0.2% arabinose for 2 hours. Middle and right panels show the growth of the uninduced or induced *pYtopA-R327W* transformants, respectively. The dilution of each sample is indicated above the images. Columns of equal spotting densities are indicated by red circles. Representative plates of duplicates are shown. (D) Growth of *pYtopA-R327W* transformants under continuous induction with the indicated concentrations of arabinose. Representative plates of duplicates are shown.

strains proficient or deficient in ExoVII (wild-type, $\Delta xseA$, or $\Delta xseB$) with a single-copy plasmid carrying *gyrA-S83L* (*pgyrA-S83L*) (17–19), followed by inactivation of the genomic copy of *gyrA* (fig. S1C). As expected, the mutation *gyrA-S83L* led to resistance to ciprofloxacin, reflected by a 10-fold increase in ciprofloxacin MIC (compare Fig. 1, A and B). Inactivating either subunit of ExoVII in the *gyrA-S83L* strain resensitized the bacteria to quinolones by ~2-fold (Fig. 1B and fig. S1D) (12, 21), demonstrating the functional importance of ExoVII in the quinolone-resistant bacteria strains.

The other major topoisomerases in prokaryotes are type IA topoisomerases, which also form transient covalent bond to the 5'-end of DNA but change DNA topology by generating DNA single-strand breaks rather than concerted DNA double-strand breaks (8, 22, 23). To examine whether ExoVII also plays a role in repairing type IA TOPcc, we induced expression of a mutated type IA topoisomerase, *Yersinia pestis* topoisomerase I-R327W (YTop1-R327W), that leads to accumulation of toxic covalently linked Top1 (22, 24). We used *Y. pestis* Top1 (encoded by *YtopA*) because it shares ~85% sequence

identity with *E. coli* Top1, yet the clone with the dominant lethal mutant *YtopA* is more stable (22). In both ExoVII-proficient and ExoVII-deficient strains (WT, $\Delta xseA$, and $\Delta xseB$), induction of the control empty vector or WT YTop1 by arabinose showed comparable growth to the uninduced YTop1-R327W cells (Fig. 1C and fig. S2). By contrast, induction of YTop1-R327W decreased survival by more than 1000-fold (Fig. 1C and fig. S2), confirming the detrimental effects of YTop1-R327W. Notably, we did not observe any additional growth defects in the ExoVII-deficient strains. We also did not observe any difference in growth rates between the WT and ExoVII-deficient strains when YTop1-R327W was continuously induced by arabinose (Fig. 1D). These results suggest that ExoVII is involved in the repair of trapped type IIA but not type IA topoisomerases in bacteria.

ExoVII removes 5'-tyrosyl adducts mimicking trapped type IIA topoisomerase

To examine whether ExoVII shares biochemical attributes similar to eukaryotic TDP enzymes for excision of tyrosyl-DNA linkages, we conducted biochemical assays with recombinant ExoVII. We first tested whether ExoVII could excise tyrosine adducts on the 5'-end of DNA, which is a mimetic of trapped type IIA TOPcc. DNA substrates were internally radiolabeled and contained phosphorothioate linkages at their 3'-ends to track only the potential excision activity of ExoVII for DNA 5'-ends. ExoVII was capable of removing the tyrosine adduct from a 4-nucleotide (nt) overhang at the 5'-end of DNA (Y-40) (Fig. 2A). We refer to this activity of ExoVII as the tyrosyl nuclease activity since it was specific for the tyrosine adducts on the 5'-end, and ExoVII did not cleave constructs bearing 5'-phosphate or 5'-hydroxyl groups (Fig. 2A). Alkaline phosphatase (CIP) treatment of the ExoVII cleavage product resulted in an upper shift (Fig. 2B), corresponding to the conversion of the terminal 5'-phosphate group into a 5'-hydroxyl group. Therefore, our biochemical analysis shows that the tyrosyl nuclease activity of ExoVII converted the Y-40 substrate into a 39-nt product with a 5'-phosphate group (Fig. 2B). The structures of the DNA constructs and ExoVII-specific cut site are shown in Fig. 2C.

After demonstrating that ExoVII could excise tyrosine adducts on 5'-DNA ends, we compared the tyrosyl nuclease activity of ExoVII for a series of DNA substrates with tyrosine adducts on varying length of 5'-overhangs (Fig. 2D). The tyrosyl nuclease activity of ExoVII was detected only with an overhang of 4 nt or more, as ExoVII was inactive for substrates with 2-nt overhangs or blunt ends (Fig. 2D). Incidentally, trapped type IIA topoisomerase in the cells is expected to be linked to the 5'-end of DNA with a 4-nt overhang (8, 25). We also found that the tyrosyl nuclease activity of ExoVII generated the same major products from substrates with either 4- or 6-nt overhangs (39-nt product with 5'-phosphate; Fig. 2D). In addition, ExoVII generated a shorter minor product in the case of 6-nt overhangs, suggesting that longer overhangs potentially confer higher processivity of ExoVII, consistent with its previously established exonuclease activity for single-stranded substrate (26). We verified that ExoVII enzyme from another independent source showed the same *in vitro* biochemical properties revealed here (fig. S3A).

To compare ExoVII's tyrosyl nuclease activity with its single-stranded exonuclease activity, we tested the activity of ExoVII for 5'-tyrosine on a 4-nt overhang versus a substrate with 5-nt overhang (fig. S3B), where the single-stranded regions of the two substrates are comparable in length. ExoVII processed both substrates

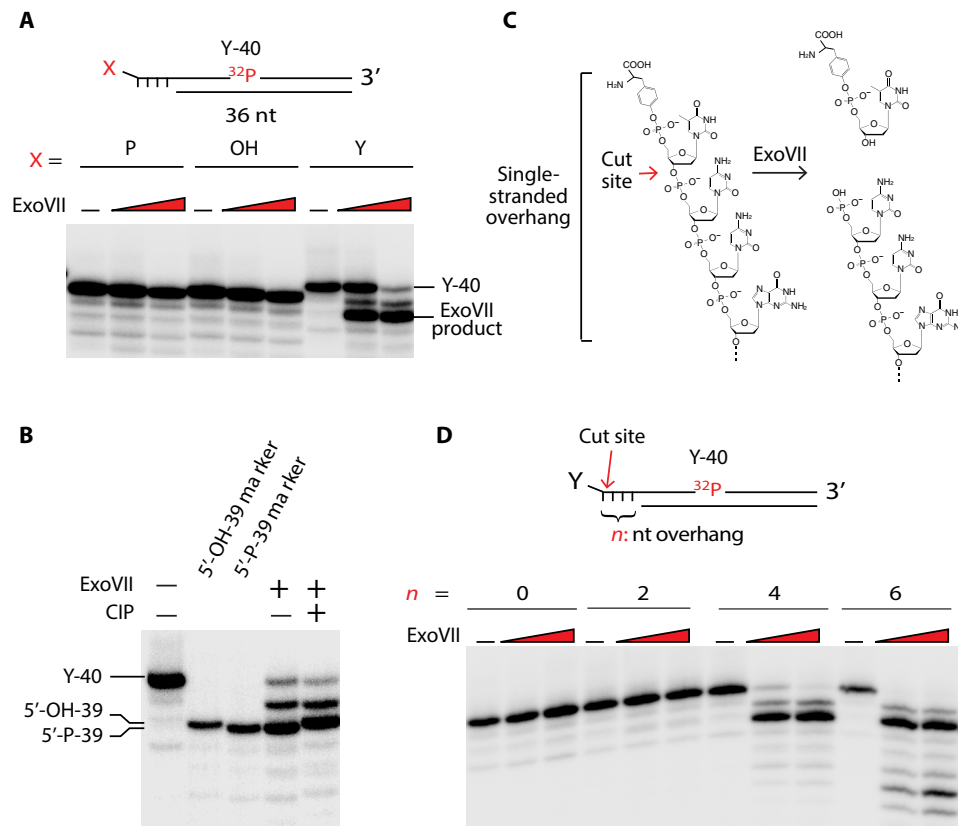


Fig. 2. Recombinant ExoVII shows selective tyrosyl nuclease activity for tyrosyl-DNA linkages on 5'-overhangs. (A) The upper strands of all three DNA constructs were internally radiolabeled. The constructs differ only by the terminal chemical group of the 5'-overhangs, phosphate (X=P), hydroxyl (X=OH), or phosphotyrosine (X=Y). Concentrations of ExoVII ranged from 0.033 to 0.1 U/ μ l. The DNA cleavage products were resolved on a 20% denaturing polyacrylamide gel electrophoresis (PAGE). A representative gel of three independent experiments is shown. (B) The tyrosyl nuclease activity of ExoVII processes the Y-40 construct [same as in (A)] to generate a 39-nt product bearing a 5'-phosphate. Treatment of ExoVII-generated product with alkaline phosphatase (CIP) removes the 5'-phosphate, as demonstrated by the two 39-nt markers bearing either a 5'-phosphate or 5'-hydroxyl group. Note that the oligo bearing an additional phosphate group travels faster in PAGE. (C) Scheme of the specific cleavage activity of ExoVII for 5'-tyrosine adducts. The single-stranded overhang regions and the site of ExoVII cleavage are indicated (red arrow). (D) The length of the 5'-overhangs influences the tyrosyl nuclease activity of ExoVII. Constructs differed only in the complementary lower strands, resulting in 5'-overhangs with different lengths. Concentrations of ExoVII ranged from 0.033 to 0.1 U/ μ l. A representative gel of five independent experiments is shown.

similarly, with a slightly higher efficiency for the tyrosine adducts (fig. S3, B and C). We also compared DNA constructs with varying lengths in their duplex regions. The tyrosyl nuclease efficiency of ExoVII increased with DNA constructs containing longer duplex regions (fig. S4, A and B). The fact that longer duplex regions lead to higher cleavage efficiencies of ExoVII suggests a mechanism where ExoVII likely could bind and scan the duplex DNA before locating its single-stranded cleavage substrates at the end.

The other major class of topoisomerase, type IB topoisomerases, is largely absent from the bacterial domain with the exception of a handful of species (27, 28). While type IA and type IIA topoisomerases form cleavage complexes on the 5'-end of DNA, type IB topoisomerase forms cleavage complex on the 3'-end of DNA. To further define the substrate specificity of ExoVII, we tested the tyrosyl nuclease activity of ExoVII for tyrosine adducts on 3'-DNA overhangs. As expected, because of its exonuclease activity, ExoVII degraded DNA substrates with 3'-overhangs but not the substrates with blunt ends. Furthermore, ExoVII degraded substrates with tyrosine adducts on 3'-overhangs to the same degree as the substrates bearing a phosphate or a hydroxyl group on the 3'-overhangs (fig. S5A). We conclude that the presence of a tyrosine adduct on the

3'-overhangs has no impact on the 3'-single-stranded exonuclease activity of ExoVII.

To complete our biochemical analyses, we tested ExoVII activity for tyrosine adducts on 5'-overhangs of RNA because type IA topoisomerases have been shown to act as RNA topoisomerases (29, 30). We could not detect any ExoVII tyrosyl nuclease activity for tyrosine-RNA linkages (fig. S5B). In addition, because ExoVII is known to cleave single-stranded DNA and type IIA topoisomerase can generate single-strand breaks (8), we compared the ExoVII exonuclease efficiency for single-stranded DNA with or without the 5'-tyrosine adducts. The exonuclease activity of ExoVII was similar for both substrates (fig. S5C). Together, these results demonstrate the specificity of ExoVII tyrosyl nuclease activity for substrates derived from type IIA TOPcc. Consistent with the tyrosyl nuclease activity of ExoVII reported here, a recent study used ExoVII to construct libraries for the purpose of genome-wide mapping of trapped TOP2 sites by END-seq (31).

ExoVII-deficient *E. coli* strains accumulate more ciprofloxacin-induced trapped DNA gyrase

To establish the tyrosyl nuclease activity of ExoVII in bacteria, we reasoned that inactivating ExoVII would lead to increased accumulation

of trapped DNA gyrase on genomic DNA. To facilitate the detection of trapped DNA gyrase *in vivo*, we introduced a C-terminal His-tagged GyrA on a single-copy plasmid (*pgyrA_{His}*) into WT, $\Delta xseA$, and $\Delta xseB$ *E. coli* strains. As expected, only transformants of *pgyrA_{His}* showed detectable GyrA_{His} expression (fig. S6A). Immunoblots probed with anti-GyrA antibodies confirmed that the exogenous GyrA_{His} was expressed at levels close to that of endogenous GyrA to minimize any potential perturbations caused by exogenous expression of GyrA (fig. S6B). All transformants displayed similar levels of sensitivity to quinolones and comparable MIC for ciprofloxacin as the nontransformed strains (figs. S6, C and D, S1, A and B; and Fig. 1A).

Using these transformant strains in a modified rapid approach to DNA adduct recovery (RADAR) assay (fig. S7A) (32–34), we detected trapped DNA gyrase on genomic DNA *in vivo* upon ciprofloxacin treatment in a dose-dependent manner (fig. S7B). Having optimized the RADAR assay, we measured trapped DNA gyrase levels in different transformant strains after a 6-hour treatment with clinical plasma concentration of ciprofloxacin (~0.5 $\mu\text{g/ml}$) (35). ExoVII-deficient transformant strains ($\Delta xseA$ -*pgyrA_{His}* and $\Delta xseB$ -*pgyrA_{His}*) accumulated significantly more trapped DNA gyrase than the WT transformant strain (WT-*pgyrA_{His}*) (Fig. 3, A and B). The levels of DNA in each sample probed with anti-DNA antibody served as loading controls. The enhanced accumulation of trapped DNA gyrase correlated with the decreased survival rates of the ExoVII-deficient transformant strains (fig. S8A). The ExoVII-deficient strains also showed hypersensitivity to ciprofloxacin even with relatively short treatments (fig. S8B). Combined, these results support the conclusion that ExoVII is directly involved in the repair of trapped DNA gyrase *in vivo*.

Denaturation of trapped DNA gyrase is required for ExoVII-mediated excision

The eukaryotic TDP enzymes cannot efficiently excise TOPcc unless the TOPcc is first unfolded or digested (10, 36–41). Hence, we examined whether the tyrosyl nuclease activity of ExoVII is capable of excising native trapped DNA gyrase generated with recombinant DNA gyrase and radiolabeled DNA substrates. In the presence of ciprofloxacin, the majority of DNA substrate (30 nt long) became retained in the wells of sequencing gels as a result of covalent attachment to the DNA gyrase (fig. S9). The addition of ExoVII failed to resolve the DNA gyrase TOPcc and to release the DNA from the wells (fig. S9), indicating that ExoVII is unable to process native intact DNA gyrase cleavage complexes.

To test whether ExoVII could process denatured DNA gyrase TOPcc, we isolated the DNA gyrase TOPcc with the RADAR assays, where the polypeptide chains of the DNA gyrase TOPcc are denatured by guanidinium isothiocyanate. Similar to the prior biochemical experiments, the DNA gyrase TOPcc cannot enter the polyacrylamide gels unless the covalently linked DNA is first digested away. Upon complete digestion of the genomic DNA, the released DNA gyrase can subsequently enter the polyacrylamide gels and become detectable by immunoblots (untreated versus benzonase-treated samples, Fig. 3C). Treating the denatured DNA gyrase TOPcc with ExoVII also led to the release of full-length DNA gyrase (detected in immunoblot in Fig. 3C), demonstrating that ExoVII can excise covalently-linked DNA gyrase from DNA when the peptide is denatured, similar to eukaryotic TDP enzymes.

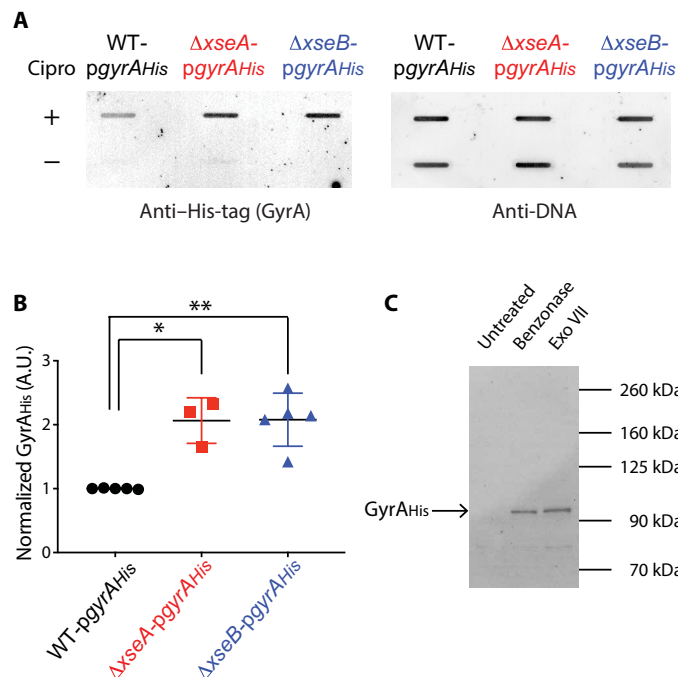


Fig. 3. ExoVII-deficient *E. coli* strains accumulate trapped DNA gyrase upon ciprofloxacin treatment. (A) *E. coli* WT and strains deficient in either subunit of ExoVII, $\Delta xseA$ or $\Delta xseB$ were transformed with a single-copy plasmid bearing *gyrA* with a C-terminal His-tag (*pgyrA_{His}*). Each transformant strain was grown to log phase and subjected to 6-hour treatment with ciprofloxacin at 0.5 $\mu\text{g/ml}$. Bacteria were lysed to extract their genomic DNA. Equal amounts of DNA were spotted onto polyvinylidene difluoride (PVDF) membrane and probed with indicated antibodies. Immunoblotting with antibodies for DNA served as a loading control. (B) Quantification of trapped GyrA_{His}. The intensity of anti-His-tag band from each sample in (A) was corrected for the amount of input DNA, measured by the intensity of the respective anti-DNA band. The adjusted GyrA_{His} signals were then normalized to the signal of the WT strain, set as 1. Statistical significance was calculated using two-tailed Mann-Whitney test in GraphPad Prism. * $P < 0.05$. ** $P < 0.01$. A.U., arbitrary units. (C) Immunoblotting of purified *E. coli* (*pgyrA_{His}*) genomic DNA from RADAR assays after ciprofloxacin treatment. *E. coli* genomic DNA samples were either untreated, treated with benzonase or with ExoVII (1 U/ μl) at 37°C for 2 hours, and then resolved by tris-glycine-SDS-PAGE and probed with anti-His-tag antibodies. A representative blot of three independent experiments is shown.

ExoVII inhibitor synergizes with ciprofloxacin

While quinolones are widely used in the clinic, drug resistance among pathogenic bacteria has become increasingly frequent (42). While higher concentrations of quinolones might exert antimicrobial effects on the quinolone resistance strains, it is often limited by adverse side effects in patients. Because our study (see Fig. 1) and previous publications (11, 12, 14–16) show that genetic inactivation of ExoVII leads to hypersensitization to quinolones, including in the quinolone-resistant *E. coli* strains, we hypothesize that chemical inhibitors of ExoVII could serve as “helper drugs” and enhance the efficacy of quinolones in the resistant strains that are otherwise difficult to eradicate in patients.

To that end, we conducted a focused screen for ExoVII inhibitors that could synergize with quinolones in the quinolone-resistant strain (WT-*pgyrA*-S83L). We identified 7-(3-chlorophenyl)-1,3(2*H*,4*H*)-isoquinolinedione (CPID) (Fig. 4A) from a family of isoquinolinedione compounds that was previously shown to inhibit human TDP2 *in vitro* but did not synergize with etoposide (eukaryotic type

IIA topoisomerase poison) in cultured cells (43). We found that CPID was highly synergistic with ciprofloxacin in the quinolone-resistant strain (WT-*pgyR*A-S83L) (Fig. 4B), while it was not synergistic in the ExoVII-deficient strains (Δ *xseA*-*pgyR*A-S83L or Δ *xseB*-*pgyR*A-S83L), suggesting that CPID acts as a specific inhibitor of ExoVII (Fig. 4C). Consistent with this possibility, in vitro biochemical assays showed that CPID inhibited ExoVII with an average IC₅₀ (half-maximal inhibitory concentration) of 2.4 μ M (Fig. 4D), while it failed to show inhibitory activity against human TDP1 (43). CPID also showed relatively low toxicity in two cell lines, human embryonic kidney (HEK) 293 cells, and murine embryonic fibroblasts (MEFs) at concentrations up to 100 μ M after a 72-hour treatment (Fig. 4E). Combined, these results provide the proof of principle that successful development of ExoVII inhibitors could help in mitigating the threat of bacteria strains resistant to quinolones.

DISCUSSION

The DNA repair function of ExoVII uncovered here establishes ExoVII as a prokaryotic functional analog of eukaryotic TDP2. It

is the first DNA-tyrosyl phosphodiesterase activity reported for the bacterial domain, providing the missing link accounting for the hypersensitivity of ExoVII-deficient strains to quinolones (11, 12, 14–16, 21). ExoVII-mediated repair pathway, similar to eukaryotic TDP-mediated pathways, likely evolved to resolve basal levels of trapped type IIA TOPcc. Yet, topoisomerase poisons can lead to markedly elevated levels of TOPcc such that the repair pathways become overwhelmed, which is why these therapeutics have strong anticancer or antimicrobial effects. Nevertheless, the biological importance of ExoVII is underscored by its conservation across the entire bacterial domain and in some archaea species as well (44). A recent study also showed that, in response to quinolones, the XseA subunit of ExoVII is activated by MarA, a transcription factor associated with the multiple antibiotic resistance (*mar*) operon in *E. coli* (15), further substantiating the significance of ExoVII in antimicrobial resistance.

ExoVII is known to efficiently degrade single-stranded DNA, including the single-stranded regions of DNA overhangs (13). Our biochemical assays with ExoVII indicate that single-stranded overhang regions shorter than 4 nt are refractory to ExoVII cleavage,

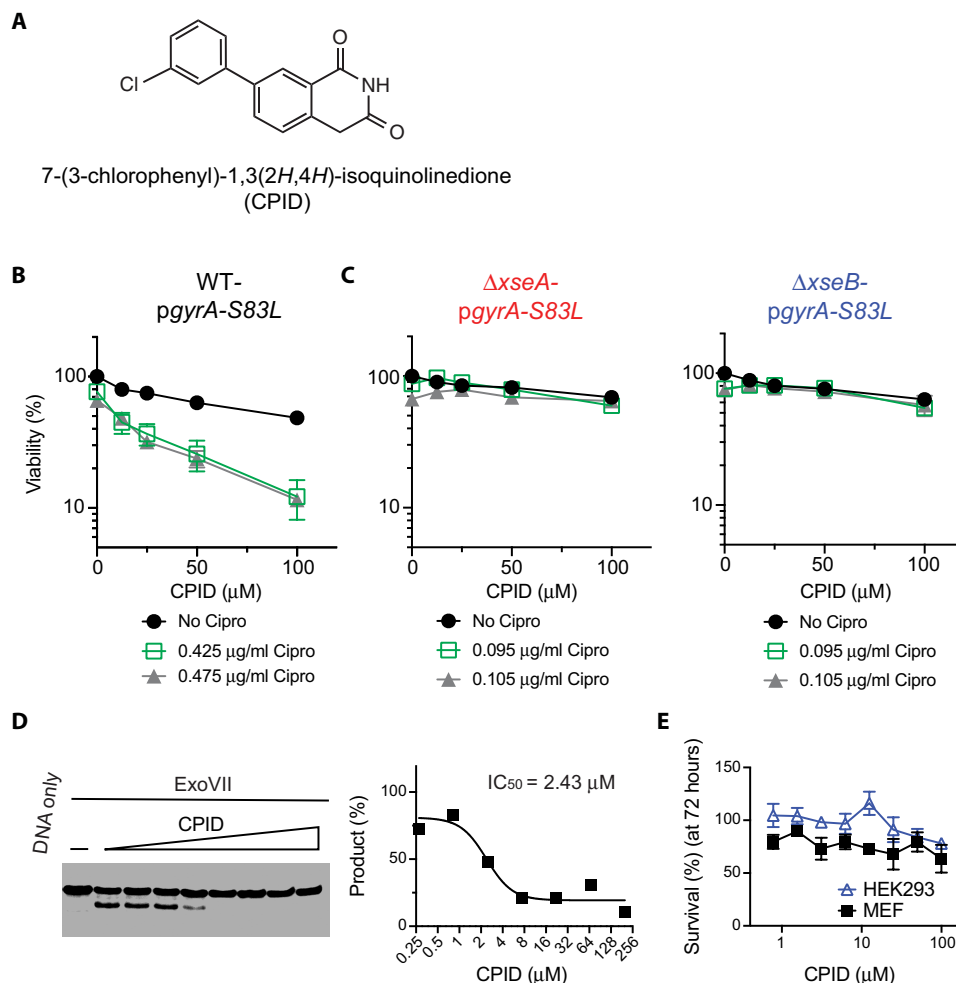


Fig. 4. CPID is a specific ExoVII inhibitor. (A) Chemical structure of 7-(3-chlorophenyl)-1,3(2H,4H)-isoquinolinedione (CPID). (B) CPID shows synergistic effect with ciprofloxacin in a quinolone-resistant strain, WT-*pgyR*A-S83L. (C) CPID does not synergize with ciprofloxacin in the quinolone-resistant strains deficient in either subunit of ExoVII. (D) In vitro cleavage assay showing inhibition of ExoVII activity in a dose-dependent manner. Representative gel image and quantification are shown. IC₅₀ value was averaged from five independent experiments. (E) CPID is not toxic to HEK293 or MEF cells as determined by relative confluency of seeded cells after 72-hour treatment at the indicated CPID concentration ($n = 3$; error bars represent SEM).

while ExoVII exonuclease activity becomes increasingly processive with longer single-stranded regions. We show that DNA substrates with overhangs longer than 4 nt, including the tyrosine moiety linked to a 4-nt overhang, are efficiently digested by ExoVII. The activity of ExoVII appears to be fine-tuned so that it is primed for DNA adducts at the end of 4-nt overhangs, which correspond to trapped type IIA TOPcc in vivo (8, 25). We also found that ExoVII can remove DNA gyrase from trapped TOPcc under conditions where the polypeptide is denatured, similar to previous findings for the eukaryotic TDP1 and TDP2 (36–41). These observations suggest that the substrate binding site of ExoVII is large enough to accommodate the denatured type IIA topoisomerase polypeptide covalently attached to single-stranded 5'-DNA ends.

Prokaryotic type IIA topoisomerases consist of DNA gyrase and topoisomerase IV (Topo IV), where the two ubiquitous enzymes have complementary yet partially overlapping biological functions (42, 45). Here, we show that ExoVII directly excises DNA gyrase TOPcc induced by quinolones, but quinolones actually trap both DNA gyrase and Topo IV (42). In *E. coli*, a Gram-negative bacterium, trapped DNA gyrase is the main source of quinolone-induced DNA damage. The leading quinolone-resistant mutation on *E. coli* DNA gyrase (*gyrA-S83L*) leads to decreased binding of quinolone to DNA gyrase. Yet, in the *gyrA-S83L* strain, either a second mutation on the DNA gyrase or a separate mutation on Topo IV can lead to further quinolone resistance (42). Therefore, at higher quinolone concentrations, the mutated DNA gyrase (GyrA-S83L) is still trapped by quinolones, and Topo IV TOPcc contributes to quinolone-induced cell death. In addition, inactivation of ExoVII in Gram-positive bacteria also leads to hypersensitization to quinolones (21). Since Topo IV is the primary target of quinolones in Gram-positive bacteria, ExoVII likely plays a role in the repair of Topo IV TOPcc as well.

Current U.S. Food and Drug Administration (FDA) guidance reserves the use of quinolones for the most serious bacterial infections due to their associated side effects and to limit the occurrence of drug-resistant bacterial strains. Considering the role of ExoVII in repairing quinolone-induced DNA damage, it is possible that lower doses of quinolones combined with an ExoVII inhibitor could achieve sufficient clinical benefits, thus decreasing the adverse side effects of quinolones. Furthermore, in the case that bacterial strains develop resistance to quinolones, ExoVII inhibitors may help to partially restore the sensitivity to quinolones. The emergence of multidrug- and pandrug-resistant bacterial strains poses a health threat across the world. Yet, no new classes of antibiotics have been approved by the FDA in nearly two decades. In this context, our drug screen provides the proof of principle that ExoVII could be targeted to boost the efficacy of quinolones and potentially overcome resistance to quinolones while limiting their side effects (46).

Because the substrates for ExoVII and TDP2 share significant structural similarities (both repair enzymes resolve trapped type IIA topoisomerases), it is plausible that some inhibitors can be effective for both enzymes. One such example revealed here is CPID, which belongs to a family of isoquinolinedione compounds. CPID was previously reported to inhibit TDP2 in vitro (47), and here, we demonstrate its inhibitory effect on ExoVII both in vitro and in vivo. Notably, the strongest known TDP2 inhibitor (SV-5-153) failed to inhibit ExoVII (our unpublished results), indicative of additional undefined differences between ExoVII and TDP2. While further studies on the class of isoquinolinedione compounds as ExoVII inhibitors are warranted, structural studies on the multimeric ExoVII

will help elucidate any mechanistic difference with TDP2, a simpler monomeric enzyme (48, 49).

MATERIALS AND METHODS

Generation of *E. coli* strains

Details of the *E. coli* strains used in this study are listed in Table 1. All DNA primers used were obtained from Integrated DNA Technologies (IDT) with their sequences listed in Table 2. The parental strains (WT, $\Delta xseA$, and $\Delta xseB$) were obtained from Coli Genetic Stock Center at the Yale University. The complete *gyrA* gene including its endogenous promoter and a C-terminal His-tag was cloned from the genomic DNA of *E. coli* K-12 MG1655 strain using *gyrA*_{His} forward primer (FP) and backward primer (BP) and introduced into single-copy plasmid pBeloBac11 [New England Biolabs (NEB)] at Bam HI and Hind III sites using In-Fusion (TaKaRa). The plasmids bearing *gyrA*_{His} (*pgyrA*_{His}) were used to transform into the three parental strains using Transformation & Storage Solution (TSS) transformation protocol and selected on Lysogeny Broth (LB, 10 g salt)-chloramphenicol (Cm) (10 μ g/ml). Transformants were verified with immunoblotting. To generate quinolone-resistant strains, mutation *gyrA-S83L* was introduced into the same plasmid using QuikChange Lightning (Agilent) and *gyrA-S83L* FP and BP before establishing transformants. To delete the genomic copy of *gyrA*, we first transformed a derivative of WT *E. coli* MG1655 carrying the lambda Red recombineering functions with *pgyrA*_{His}, selected on LB-Cm (10 μ g/ml) and purified once on the same media at 32°C. A transformant was grown in 10 ml of LB-Cm (10 μ g/ml) at 32°C to an OD₆₀₀ (optical density at 600 nm) of 0.6, and Red function expression was induced for 15 min at 42°C. Cells were centrifuged and washed four times in ice-cold sterile water and electroporated with 100 ng of a *zeo*^R cassette containing 40–base pair (bp) homologies upstream and downstream of *gyrA* generated by polymerase chain reaction (PCR) with *gyrA*-KO-*zeo*-FP and BP. After a 1-hour recovery in 1 ml of LB, chromosomal *gyrA* knockout clones were selected on LB plates in the presence of Cm (10 μ g/ml) and Zeo (25 μ g/ml) and incubated at 37°C overnight. Colonies were purified thrice more, and the disruption of genomic *gyrA* was verified by PCR using primers *gyrA*-KO-FP and BP. A P1 lysate was generated from the knockout cells, and P1 transduction was carried out on cells carrying pBeloBac-*gyrA-S83L*_{his}, as described previously (50). The disruption of the genomic *gyrA* in these strains was verified by PCR using primers *gyrA*-KO-FP and BP. *pYtopA* and *pYtopA-R327W* were generated using pBAD/TOPO ThioFusion Expression Kit (Thermo Fisher Scientific), as previously described (24), and transformants of all three plasmids in the parental strains were obtained using TSS transformation protocol and selected with Ampicillin (100 μ g/ml).

Spotting and cell killing assays

Exponentially growing *E. coli* cultures were diluted to OD₆₀₀ of 10⁻⁶, then 5 μ l of fivefold serial dilution was spotted onto LB plates containing indicated concentration of ciprofloxacin or nalidixic acid, and incubated at 37°C overnight. For determination of MIC of ciprofloxacin, 200 μ l of exponentially growing culture (OD₆₀₀ = 10⁻¹) was plated on LB plates, then the MIC ciprofloxacin test strips (Liofilchem) were applied to the plates, and incubated at 37°C overnight following the manufacturer's instruction. Cell-killing assays were carried out as previously described (22). Briefly, transformants

AQ24

Table 1. List of strains.

Name	Genotype	Source
WT	BW25113	Yale Coli Genetic Stock Center
$\Delta xseA$	BW25113 $\Delta xseA::Kn$. Kan ^R	Yale Coli Genetic Stock Center
$\Delta xseB$	BW25113 $\Delta xseB::Kn$. Kan ^R	Yale Coli Genetic Stock Center
NM1100	MG1655 mini $\lambda::tet$, recombinering strain	Current study
NM50000	NM1100 pBeloBac- <i>gyrA</i> _{his} recombinered with $\Delta gyrA::zeo$. Cm ^R Zeo ^R Tet ^S	Current study
WT-pgyrA-S83L	BW25113 pBeloBac- <i>gyrA</i> -S83L _{his} transduced with $\Delta gyrA::zeo$ from NM50000. Cm ^R Zeo ^R	Current study
$\Delta xseA$ -pgyrA-S83L	BW25113 $\Delta xseA::Kn$ pBeloBac- <i>gyrA</i> -S83L _{his} transduced with $\Delta gyrA::zeo$ from NM50000. Cm ^R Zeo ^R	Current study
$\Delta xseB$ -pgyrA-S83L	BW25113 $\Delta xseB::Kn$ pBeloBac- <i>gyrA</i> -S83L _{his} transduced with $\Delta gyrA::zeo$ from NM50000. Cm ^R Zeo ^R	Current study
WT-pBAD/Thio	BW25113 pBAD/Thio. Amp ^R	Current study
$\Delta xseA$ -pBAD/Thio	BW25113 $\Delta xseA::Kn$ pBAD/Thio. Amp ^R	Current study
$\Delta xseB$ -pBAD/Thio	BW25113 $\Delta xseB::Kn$ pBAD/Thio. Amp ^R	Current study
WT-pYtopA	BW25113 pBAD/Thio-YtopA. Amp ^R	Current study
$\Delta xseA$ -pYtopA	BW25113 $\Delta xseA::Kn$ pBAD/Thio-YtopA. Amp ^R	Current study
$\Delta xseB$ -pYtopA	BW25113 $\Delta xseB::Kn$ pBAD/Thio-YtopA. Amp ^R	Current study
WT-pYtopA-R327W	BW25113 pBAD/Thio-YtopA-R327W. Amp ^R	Current study
$\Delta xseA$ -pYtopA-R327W	BW25113 $\Delta xseA::Kn$ pBAD/Thio-YtopA-R327W. Amp ^R	Current study
$\Delta xseB$ -pYtopA-R327W	BW25113 $\Delta xseB::Kn$ pBAD/Thio-YtopA-R327W. Amp ^R	Current study
WT-pgyrA _{his}	BW25113 pBeloBac- <i>gyrA</i> _{his} . Cm ^R	Current study
$\Delta xseA$ -pgyrA _{his}	BW25113 $\Delta xseA::Kn$ pBeloBac- <i>gyrA</i> _{his} . Cm ^R	Current study
$\Delta xseB$ -pgyrA _{his}	BW25113 $\Delta xseB::Kn$ pBeloBac- <i>gyrA</i> _{his} . Cm ^R	Current study

Table 2. List of primers.

Name	Sequence
<i>gyrA</i> _{his} FP	5'-CGGTACCCGGGATCCGGATGTGAATAAAGCGTATAGG
<i>gyrA</i> _{his} BP	5'-TAGAATACTCAAGCTTTTGTGGTGTGGTGTATGTTCTTCTCTGGCTCGTCGTCACACG
<i>gyrA</i> -S83L FP	5'-CATGGTGACTTGGCGGTCTAT
<i>gyrA</i> -S83L BP	5'-ATAGACCGCCAAGTCACCATG
<i>gyrA</i> -KO-zeo-FP	5'-TACTCCGTAATTGGCAAGCAAACGAGTATATCAGGCATTGTTGACAATTAATCATCGGG
<i>gyrA</i> -KO-zeo-BP	5'-AAGGGAGATAGCTCCCTTTTGGCATGAAGAAGTAAAATTATCAGTCTGCTCCCTCGGCCA
<i>gyrA</i> -KO-FP	5'-TCATTGGCACTTCTACTCCG
<i>gyrA</i> -KO-BP	5'-AAGGGAGATAGCTCCCTTTT

harboring pBAD/Thio, pYtopA or pYtopA-R327W, were grown in LB with 2% glucose and carbenicillin (50 μ g/ml) overnight and diluted 1:100 in LB with carbenicillin (50 μ g/ml) and grown to OD₆₀₀ of 0.4. YTop1 or YTop1-R327W was induced by the addition of 0.2% arabinose for 0.5 to 2 hours. Postinduction cultures were then serially diluted and spotted onto LB plates with 2% glucose and carbenicillin (50 μ g/ml) and incubated at 37°C overnight. Alternatively, exponentially growing transformants were serially

diluted as indicated and spotted on LB plates containing carbenicillin (50 μ g/ml) and indicated concentrations of arabinose and incubated at 37°C overnight.

Screen for ExoVII inhibitor

Exponentially growing WT-pgyrA-S83L, $\Delta xseA$ -pgyrA-S83L, or $\Delta xseA$ -pgyrA-S83L at OD₆₀₀ of 3×10^{-4} was combined with equal volume of media containing indicated inhibitor concentrations

with or without ciprofloxacin at indicated concentrations in clear-bottom 96-well plates. OD₆₀₀ was measured at the end of 4-hour incubation at 37°C shaking at 225 rpm, and cell densities were normalized to samples without any drug treatment. Toxicity of compounds was measured by treating either HEK293 or MEF cells (1000 cells in 96-well plates seeded 24 hours prior) with indicated concentrations of ExoVII inhibitor for 72 hours. The samples were imaged with a Cytation 5 (BioTek), and the confluency of each well was normalized to untreated samples.

Generation of DNA constructs and biochemical assays

The biochemical constructs for ExoVII activity were generated as described previously (31). All oligonucleotides were synthesized by IDT or Midland, and all sequences of DNA oligos are listed in Table 3. For the series of constructs with different chemical groups on 5'-overhangs, a 22-nt DNA with three phosphorothioate bonds on the 3'-ends (T-22-3PT) was labeled with ³²P at the 5'-end with [γ -³²P]ATP (adenosine triphosphate) (PerkinElmer Life Sciences) and T4 polynucleotide kinase (NEB) and then purified by mini

Quick Spin Oligo Columns (Sigma-Aldrich). An 18-nt DNA harboring different chemical groups at the 5'-end (P-18, OH-18, or Y-18) was mixed with the 5'-labeled T-22-3PT before annealing to a complementary strand between 34 and 40 nt long (B-34, B-36, B-38, and B-40) at 1:1:1 ratio. The nicks were sealed with T4 DNA ligase (NEB). For constructs longer than 40 bp, an additional middle piece (M-20 or M-40) was also included in the annealing reaction, with the appropriate complementary strands (B-56 or B-76) before ligation to generate Y-60 and Y-80, each with 4-nt 5'-overhangs. To generate Y-19 with 4-nt 5'-overhangs, Y-18 was labeled on the 3'-end with [α -³²P] cordycepin and terminal transferase (NEB), then purified by mini Quick Spin Oligo Columns (Sigma-Aldrich), and annealed to B-15 at 1:1 ratio. To generate RNA constructs with 5'-phosphotyrosine, T-22-3PT was labeled with ³²P at the 5'-end as described before, mixed with Y-10-DNA or Y-10-RNA, before annealing to B-28 or B-32 at 1:1:1 ratio in the presence of RNasin Plus (3 U/ μ l; Promega). For the series of constructs with different chemical groups on 3'-overhangs, a 14-nt DNA harboring different chemical groups at the 3'-end (14-P, 14-OH, or 14-Y) was labeled

Table 3. List of DNA oligos.

Name	Sequence	Modification
T-22-3PT	5'-GCGCAGCTAGCGGCGGATG*G*C*A	* = phosphorothioate bond
P-18	5'-P-TCCGTTGAAGCCTGCTTT	P = phosphate
OH-18	5'-TCCGTTGAAGCCTGCTTT	
Y-18	5'-Y-TCCGTTGAAGCCTGCTTT	Y = phosphotyrosine
OH-19	5'-TTCCGTTGAAGCCTGCTTT	
B-34	5'-TGCCATCCGCCGCTAGCTGCGCAAAGCAGGCTTC	
B-36	5'-TGCCATCCGCCGCTAGCTGCGCAAAGCAGGCTTCAA	
B-38	5'-TGCCATCCGCCGCTAGCTGCGCAAAGCAGGCTTCAACG	
B-40	5'-TGCCATCCGCCGCTAGCTGCGCAAAGCAGGCTTCAACGGA	
B-15	5'-TAAAGCAGGCTTCAA	
B-56	5'-TGCCATCCGCCGCTAGCTGCGCA CTCTTGACCCTACGACGATAAAGCAGGCTTCAA	
B-76	5'-TGCCATCCGCCGCTAGCTGCGCACTCTTGACCCTAC GACGATACTCTTGACCCTACGACGATAAAGCAGGCTTCAA	
M-20	5'-P-ATCGTCGTAGGGTCAAGAGT	P = phosphate
M-40	5'-P-ATCGTCGTAGGGTCAAGAGTATCGTCGTAGGGTCAAGAGT	P = phosphate
Y-10-DNA	5'-Y-TTAAACAGC	Y = phosphotyrosine
Y-10-RNA	5'-Y-rUrUrArArArArCrArGrC	Y = phosphotyrosine
B-28	5'-TGCCATCCGCCGCTAGCTGCGCGCTGTT	
B-32	5'-TGCCATCCGCCGCTAGCTGCGCGCTGTTTTAA	
T-22	5'-GCGCAGCTAGCGGCGGATGGCA	
14-P	5'-GATCTAAAAGACTT-P	P = phosphate
14-OH	5'-GATCTAAAAGACTT	
14-Y	5'-GATCTAAAAGACTT-Y	Y = phosphotyrosine
B-32-3Y	5'-CTTTAGATCTGCCATCCGCCGCTAGCTGCGC	
B-36-3Y	5'-AAGTCTTTAGATCTGCCATCCGCCGCTAGCTGCGC	
T-22-15PT	5'-GCGCAGC*T*A*G*C*G*G*C*G*G*A*T*G*G*C*A	* = phosphorothioate bond
Gyr-1	5'-GAATCATAATGGGAAGCCATCCAGCCTC	
Gyr-2	5'-TGAGGCTGGATGGCCTTCCCATATGATTC	

with ^{32}P at the 5'-end as described before, then mixed with T-22, and annealed to B-32-3Y or B-36-3Y at 1:1:1 ratio, followed by DNA ligation. For single-stranded constructs, T-22-15PT (15 phosphorothioate bonds on the 3'-ends) was labeled with ^{32}P at the 5'-end as described before, then mixed with OH-18 or Y-18 at 1:1 ratio, and ligated with T4 RNA Ligase 1 (NEB) following the manufacturer's instructions. For generation of *E. coli* DNA gyrase cleavage complexes, Gyr-1 was labeled on the 3'-end with [α - ^{32}P] cordycepin and terminal transferase (NEB), then purified by mini Quick Spin Oligo Columns (Sigma-Aldrich), and annealed to Gyr-2 at 1:1 ratio.

Reactions with ExoVII (Thermo Fisher Scientific or NEB) were performed in 10 μl of reaction containing 20 to 100 nM internally radiolabeled DNA substrate and indicated concentration of ExoVII in buffer with 50 mM potassium acetate, 20 mM tris-acetate (pH 7.9), 10 mM magnesium acetate, and 1 mM dithiothreitol (DTT). ExoVII reactions were incubated at 37°C for 1 or 2 hours followed by inactivation at 55°C for 30 min before being terminated by the addition of 20 μl of formamide gel loading buffer [96% (v/v) formamide, 10 mM ethylenediaminetetraacetic acid, 1% (w/v) xylene cyanol, and 1% (w/v) bromophenol blue]. For IC₅₀ determination, ExoVII was preincubated with the inhibitor at 25°C for 5 min before the addition of equal volume of DNA solution, and the reaction continued for another 20 to 30 min. The 10 μl of reaction contained ExoVII (0.025 U/ μl), 20 to 100 nM internally radiolabeled DNA substrate, and indicated inhibitor concentration in buffer with 50 mM potassium acetate, 20 mM tris-acetate (pH 7.9), 10 mM magnesium acetate, 1 mM DTT, and 10% (v/v) dimethyl sulfoxide. The percentage of products in the presence of inhibitor was normalized to that of control reaction without any inhibitors, and the resulting plot was fitted to a nonlinear regression function in Prism. DNA gyrase was purified as previously described (51). Reactions with DNA gyrase were performed in 10 μl of reaction containing 20 to 100 nM radiolabeled DNA substrate, 40 nM DNA gyrase, and 250 nM ciprofloxacin when indicated. Reaction buffer contains 35 mM tris-HCl (pH 7.5), 24 mM KCl, 4 mM MgCl₂, 2 mM DTT, 1.7 mM spermidine, bovine serum albumin (0.36 mg/ml), 1 mM ATP, and 6.5% glycerol. After incubation at 25°C for 1 hour, ExoVII (0.375 to 1.5 U/ μl) was added, and the reactions were incubated further at 37°C for 3 hours. The reactions were stopped with 0.2% SDS and 20 μl of formamide gel loading buffer [96% (v/v) formamide, 10 mM ethylenediaminetetraacetic acid, 1% (w/v) xylene cyanol, and 1% (w/v) bromophenol blue]. All samples were heat denatured at 95°C for 5 min and analyzed by denaturing polyacrylamide gel electrophoresis (PAGE) (20%). Gels were dried and exposed on PhosphorImager screens. Imaging was done using a Typhoon 8600 imager (GE Healthcare, Little Chalfont, United Kingdom).

RADAR assays

Exponentially growing *E. coli* cells (OD₆₀₀ = 0.4) were treated with ciprofloxacin (0.5 $\mu\text{g}/\text{ml}$) for 6 hours, and then 1 ml of treated cells was directly combined with 4 ml of 1.25 \times lysis buffer [7.5 M guanidinium isothiocyanate, 12.5 mM tris-HCl (pH 6.5), 25 mM EDTA, 5% Triton X-100, and 1.25% lauroylsarcosine]. The lysates were sonicated for three cycles, each for 15 s at 60% power, and then were phenol-chloroform extracted twice. The samples were ethanol precipitated, and the DNA pellets washed twice with 80% ethanol before being air-dried. The DNA pellets were resuspended in 8 mM NaOH, and DNA concentrations of samples were quantified. Equal amount of DNA (8 μg) of each sample was blotted on polyvinylidene

difluoride (PVDF) membrane and probed with anti-His-tag rabbit monoclonal antibody (Cell Signaling) and anti-double-stranded DNA mouse monoclonal antibody (Abcam), and the band intensities were quantified by ChemiDoc System (Bio-Rad). Alternatively, 5 μg of purified DNA from ciprofloxacin-treated samples was treated with benzonase (25 U/ μl ; Millipore Sigma) or ExoVII (1 U/ μl) at 37°C for 2 hours in a buffer containing 50 mM potassium acetate, 20 mM tris-acetate (pH 7.9), 10 mM magnesium acetate, and 1 mM DTT. The samples were then resolved on a 6% tris-glycine gel, and immunoblotting was done following standard procedures and probed with anti-His-tag rabbit monoclonal antibody (Cell Signaling).

SUPPLEMENTARY MATERIALS

Supplementary material for this article is available at <http://advances.sciencemag.org/cgi/content/full/7/10/eabe0384/DC1>

[View/request a protocol for this paper from Bio-protocol.](#)

REFERENCES AND NOTES

1. K. J. Aldred, T. R. Bower, R. J. Kerns, J. M. Berger, N. Osheroff, Fluoroquinolone interactions with Mycobacterium tuberculosis gyrase: Enhancing drug activity against wild-type and resistant gyrase. *Proc. Natl. Acad. Sci. U.S.A.* **113**, E839–E846 (2016).
2. A. K. McClendon, N. Osheroff, DNA topoisomerase II, genotoxicity, and cancer. *Mutat. Res.* **623**, 83–97 (2007).
3. V. Nagaraja, A. A. Godbole, S. R. Henderson, A. Maxwell, DNA topoisomerase I and DNA gyrase as targets for TB therapy. *Drug Discov. Today* **22**, 510–518 (2017).
4. J. L. Nitiss, Targeting DNA topoisomerase II in cancer chemotherapy. *Nat. Rev. Cancer* **9**, 338–350 (2009).
5. Y. Pommier, Drugging topoisomerases: Lessons and challenges. *ACS Chem. Biol.* **8**, 82–95 (2012).
6. M. I. Andersson, A. P. MacGowan, Development of the quinolones. *J. Antimicrob. Chemother.* **51** (Suppl 1), 1–11 (2003).
7. J. F. Acar, F. W. Goldstein, Trends in bacterial resistance to fluoroquinolones. *Clin. Infect. Dis.* **24** (Suppl 1), S67–S73 (1997).
8. B. D. Bax, G. Murshudov, A. Maxwell, T. Germe, DNA topoisomerase inhibitors: Trapping a DNA-cleaving machine in motion. *J. Mol. Biol.* **431**, 3427–3449 (2019).
9. Y. Pommier, C. Marchand, Interfacial inhibitors: Targeting macromolecular complexes. *Nat. Rev. Drug Discov.* **11**, 25–36 (2011).
10. Y. Pommier, S. N. Huang, R. Gao, B. B. Das, J. Murai, C. Marchand, Tyrosyl-DNA-phosphodiesterases (TDP1 and TDP2). *DNA Repair* **19**, 114–129 (2014).
11. M. L. Henderson, K. N. Kreuzer, Functions that Protect *Escherichia coli* from Tightly Bound DNA-protein complexes created by mutant EcoRII Methyltransferase. *PLOS ONE* **10**, e0128092 (2015).
12. C. Tamae, A. Liu, K. Kim, D. Sitz, J. Hong, E. Becket, A. Bui, P. Solaimani, K. P. Tran, H. Yang, J. H. Miller, Determination of antibiotic hypersensitivity among 4,000 single-gene-knockout mutants of *Escherichia coli*. *J. Bacteriol.* **190**, 5981–5988 (2008).
13. J. W. Chase, C. C. Richardson, Exonuclease VII of *Escherichia coli*. *Basic Life Sci.* **5A**, 225–234 (1975).
14. J. W. Chase, C. C. Richardson, *Escherichia coli* mutants deficient in exonuclease VII. *J. Bacteriol.* **129**, 934–947 (1977).
15. P. Sharma, J. R. J. Haycocks, A. D. Middlemiss, R. A. Kettles, L. E. Sellars, V. Ricci, L. J. V. Piddock, D. C. Grainger, The multiple antibiotic resistance operon of enteric bacteria controls DNA repair and outer membrane integrity. *Nat. Commun.* **8**, 1444 (2017).
16. R. J. Nichols, S. Sen, Y. J. Choo, P. Beltrao, M. Zietek, R. Chaba, S. Lee, K. M. Kazmierczak, K. J. Lee, A. Wong, M. Shales, S. Lovett, M. E. Winkler, N. J. Krogan, A. Tymas, C. A. Gross, Phenotypic landscape of a bacterial cell. *Cell* **144**, 143–156 (2011).
17. S. Bagel, V. Hullen, B. Wiedemann, P. Heisig, Impact of *gyrA* and *parC* mutations on quinolone resistance, doubling time, and supercoiling degree of *Escherichia coli*. *Antimicrob. Agents Chemother.* **43**, 868–875 (1999).
18. B. C. L. van der Putten, D. Remondini, G. Pasquini, V. A. Janes, S. Matamoros, C. Schultz, Quantifying the contribution of four resistance mechanisms to ciprofloxacin MIC in *Escherichia coli*: A systematic review. *J. Antimicrob. Chemother.* **74**, 298–310 (2019).
19. B. D. Bax, P. F. Chan, D. S. Eggleston, A. Fosberry, D. R. Gentry, F. Gorrec, I. Giordano, M. M. Hann, A. Hennessy, M. Hibbs, J. Huang, E. Jones, J. Jones, K. K. Brown, C. J. Lewis, E. W. May, M. R. Saunders, O. Singh, C. E. Spitzfaden, C. Shen, A. Shillings, A. J. Theobald, A. Wohlkonig, N. D. Pearson, M. N. Gwynn, Type IIA topoisomerase inhibition by a new class of antibacterial agents. *Nature* **466**, 935–940 (2010).
20. C. Marchand, M. Abdelmalak, J. Kankanala, S.-Y. Huang, E. Kiselev, K. Fesen, K. Kurahashi, H. Sasanuma, S. Takeda, H. Aihara, Z. Wang, Y. Pommier, Deazaflavin inhibitors

- of tyrosyl-DNA phosphodiesterase 2 (TDP2) specific for the human enzyme and active against cellular TDP2. *ACS Chem. Biol.* **11**, 1925–1933 (2016).
21. M. Vestergaard, B. Leng, J. Haaber, M. S. Bojer, C. S. Vegge, H. Ingmer, Genome-wide identification of antimicrobial intrinsic resistance determinants in *Staphylococcus aureus*. *Front. Microbiol.* **7**, 2018 (2016).
 22. G. Narula, T. Annamalai, S. Aedo, B. Cheng, E. Sorokin, A. Wong, Y. C. Tse-Dinh, The strictly conserved Arg-321 residue in the active site of *Escherichia coli* topoisomerase I plays a critical role in DNA rejoining. *J. Biol. Chem.* **286**, 18673–18680 (2011).
 23. A. J. Schoeffler, J. M. Berger, Recent advances in understanding structure-function relationships in the type II topoisomerase mechanism. *Biochem. Soc. Trans.* **33**, 1465–1470 (2005).
 24. B. Cheng, S. Shukla, S. Vasunilashorn, S. Mukhopadhyay, Y.-C. Tse-Dinh, Bacterial cell killing mediated by topoisomerase I DNA cleavage activity. *J. Biol. Chem.* **280**, 38489–38495 (2005).
 25. J. C. Wang, DNA topoisomerases: Why so many? *J. Biol. Chem.* **266**, 6659–6662 (1991).
 26. J. W. Chase, C. C. Richardson, Exonuclease VII of *Escherichia coli*. Purification and properties. *J. Biol. Chem.* **249**, 4545–4552 (1974).
 27. T. Jain, B. J. Roper, A. Grove, A functional type I topoisomerase from *Pseudomonas aeruginosa*. *BMC Mol. Biol.* **10**, 23 (2009).
 28. B. O. Krogh, S. Shuman, A poxvirus-like type IB topoisomerase family in bacteria. *Proc. Natl. Acad. Sci. U.S.A.* **99**, 1853–1858 (2002).
 29. M. Ahmad, Y. Xue, S. K. Lee, J. L. Martindale, W. Shen, W. Li, S. Zou, M. Ciarabella, H. Debat, M. Nadal, F. Leng, H. Zhang, Q. Wang, G. E. Siaw, H. Niu, Y. Pommier, M. Gorospe, T. S. Hsieh, Y. C. Tse-Dinh, D. Xu, W. Wang, RNA topoisomerase is prevalent in all domains of life and associates with polyribosomes in animals. *Nucleic Acids Res.* **44**, 6335–6349 (2016).
 30. H. Wang, R. J. Di Gate, N. C. Seeman, An RNA topoisomerase. *Proc. Natl. Acad. Sci. U.S.A.* **93**, 9477–9482 (1996).
 31. A. Canela, Y. Maman, S. N. Huang, G. Wutz, W. Tang, G. Zagnoli-Vieira, E. Callen, N. Wong, A. Day, J. M. Peters, K. W. Caldecott, Y. Pommier, A. Nussenzweig, Topoisomerase II-induced chromosome breakage and translocation is determined by chromosome architecture and transcriptional activity. *Mol. Cell* **75**, 252–266.e8 (2019).
 32. S. Aedo, Y. C. Tse-Dinh, Isolation and quantitation of topoisomerase complexes accumulated on *Escherichia coli* chromosomal DNA. *Antimicrob. Agents Chemother.* **56**, 5458–5464 (2012).
 33. K. J. Aldred, A. Payne, O. Voegerl, A RADAR-based assay to isolate covalent DNA complexes in bacteria. *Antibiotics* **8**, 17 (2019).
 34. S. Aedo, Y. C. Tse-Dinh, SbcCD-mediated processing of covalent gyrase-DNA complex in *Escherichia coli*. *Antimicrob. Agents Chemother.* **57**, 5116–5119 (2013).
 35. E. J. Begg, R. A. Robson, D. A. Saunders, G. G. Graham, R. C. Buttimore, A. M. Neill, G. I. Town, The pharmacokinetics of oral fleroxacin and ciprofloxacin in plasma and sputum during acute and chronic dosing. *Br. J. Clin. Pharmacol.* **49**, 32–38 (2000).
 36. F. Cortes Ledesma, S. F. El Khamisy, M. C. Zuma, K. Osborn, K. W. Caldecott, A human 5'-tyrosyl DNA phosphodiesterase that repairs topoisomerase-mediated DNA damage. *Nature* **461**, 674–678 (2009).
 37. S.-W. Yang, A. B. Burgin, B. N. Huizenga, C. A. Robertson, K. C. Yao, H. A. Nash, A eukaryotic enzyme that can disjoin dead-end covalent complexes between DNA and type I topoisomerases. *Proc. Natl. Acad. Sci. U.S.A.* **93**, 11534–11539 (1996).
 38. S. Saha, Y. Sun, S. Huang, U. Jo, H. Zhang, Y. C. Tse-Dinh, Y. Pommier, Topoisomerase 3B (TOP3B) DNA and RNA cleavage complexes and pathway to repair TOP3B-linked RNA and DNA breaks. *Cell Rep.* **33**, 108569 (2020).
 39. H. Interthal, H. J. Chen, J. J. Champoux, Human Tdp1 cleaves a broad spectrum of substrates, including phosphoamide linkages. *J. Biol. Chem.* **280**, 36518–36528 (2005).
 40. R. Gao, M. J. Schellenberg, S.-Y. N. Huang, M. Abdelmalak, C. Marchand, K. C. Nitiss, J. L. Nitiss, R. S. Williams, Y. Pommier, Proteolytic degradation of topoisomerase II (Top2) enables the processing of Top2-DNA and Top2-RNA covalent complexes by tyrosyl-DNA-phosphodiesterase 2 (TDP2). *J. Biol. Chem.* **289**, 17960–17969 (2014).
 41. R. Gao, S. Y. Huang, C. Marchand, Y. Pommier, Biochemical characterization of human tyrosyl-DNA phosphodiesterase 2 (TDP2/TTRAP): A Mg²⁺/Mn²⁺-dependent phosphodiesterase specific for the repair of topoisomerase cleavage complexes. *J. Biol. Chem.* **287**, 30842–30852 (2012).
 42. K. Drlica, X. Zhao, DNA gyrase, topoisomerase IV, and the 4-quinolones. *Microbiol. Mol. Biol. Rev.* **61**, 377–392 (1997).
 43. J. Kankanala, C. Marchand, M. Abdelmalak, H. Aihara, Y. Pommier, Z. Wang, Isoquinoline-1,3-diones as selective inhibitors of tyrosyl DNA phosphodiesterase II (TDP2). *J. Med. Chem.* **59**, 2734–2746 (2016).
 44. K. Poleszak, K. H. Kaminska, S. Dunin-Horkawicz, A. Lupas, K. J. Skowronek, J. M. Bujnicki, Delineation of structural domains and identification of functionally important residues in DNA repair enzyme exonuclease VII. *Nucleic Acids Res.* **40**, 8163–8174 (2012).
 45. J. C. Wang, Cellular roles of DNA topoisomerases: A molecular perspective. *Nat. Rev. Mol. Cell Biol.* **3**, 430–440 (2002).
 46. M. Pieren, M. Tigges, Adjuvant strategies for potentiation of antibiotics to overcome antimicrobial resistance. *Curr. Opin. Pharmacol.* **12**, 551–555 (2012).
 47. E. Kiselev, A. Ravji, J. Kankanala, J. Xie, Z. Wang, Y. Pommier, Novel deazaflavin tyrosyl-DNA phosphodiesterase 2 (TDP2) inhibitors. *DNA Repair* **85**, 102747 (2020).
 48. K. Shi, K. Kurahashi, R. Gao, S. E. Tsutakawa, J. A. Tainer, Y. Pommier, H. Aihara, Structural basis for recognition of 5'-phosphotyrosine adducts by Tdp2. *Nat. Struct. Mol. Biol.* **19**, 1372–1377 (2012).
 49. M. J. Schellenberg, C. D. Appel, S. Adhikari, P. D. Robertson, D. A. Ramsden, R. S. Williams, Mechanism of repair of 5'-topoisomerase II-DNA adducts by mammalian tyrosyl-DNA phosphodiesterase 2. *Nat. Struct. Mol. Biol.* **19**, 1363–1371 (2012).
 50. J. H. Miller, *A Short Course in Bacterial Genetics* (Cold Spring Harbor Laboratory Press, Cold Spring Harbor, NY, 1992).
 51. A. Vanden Broeck, C. Lotz, J. Ortiz, V. Lamour, Cryo-EM structure of the complete *E. coli* DNA gyrase nucleoprotein complex. *Nat. Commun.* **10**, 4935 (2019).

Acknowledgments: We thank S. Gottesman of the NCI and A. Khare of the NCI for valuable suggestions and insightful comments. **Funding:** This work was supported by the NIH grant Z01 BC 006150 from the NCI Intramural Program, Center for Cancer Research. **Author contributions:** S.-y.N.H. designed, conducted, or supervised all experiments. S.A.M. carried out genetic and biochemical experiments. B.B.M. carried out inhibitor screen. N.M. designed and constructed bacterial strains. A.V.B. purified recombinant enzymes. A.C., Y.-C.T.-D., V.L., and Y.P. contributed to the design of experiments and interpretation of the results. S.-y.N.H. and Y.P. wrote the manuscript. **Competing interests:** S.-y.N.H., B.B.M., and Y.P. are inventors on a patent application related to this work filed by the United States of America as Represented by the Secretary, Department of Health and Human Services (no. 63129271, filed 22 December 2020). The other authors declare that they have no competing interests. **Data and materials availability:** All data needed to evaluate the conclusions in the paper are present in the paper and/or the Supplementary Materials. Additional data related to this paper may be requested from the authors.

Submitted 6 August 2020

Accepted 19 January 2021

Published 3 March 2021

10.1126/sciadv.abe0384

Citation: S.-y. N. Huang, S. A. Michaels, B. B. Mitchell, N. Majdalani, A. Vanden Broeck, A. Canela, Y.-C. Tse-Dinh, V. Lamour, Y. Pommier, Exonuclease VII repairs quinolone-induced damage by resolving DNA gyrase cleavage complexes. *Sci. Adv.* **7**, eabe0384 (2021).

Exonuclease VII repairs quinolone-induced damage by resolving DNA gyrase cleavage complexes

Shar-yin N. HuangStephanie A. MichaelsBrianna B. MitchellNadim MajdalaniArnaud Vanden BroeckAndres CanelaYuk-Ching Tse-DinhValerie LamourYves Pommier

Sci. Adv., 7 (10), eabe0384.

View the article online

<https://www.science.org/doi/10.1126/sciadv.abe0384>

Permissions

<https://www.science.org/help/reprints-and-permissions>

Use of think article is subject to the [Terms of service](#)

Science Advances (ISSN 2375-2548) is published by the American Association for the Advancement of Science. 1200 New York Avenue NW, Washington, DC 20005. The title *Science Advances* is a registered trademark of AAAS.

Copyright © 2021 The Authors, some rights reserved; exclusive licensee American Association for the Advancement of Science. No claim to original U.S. Government Works. Distributed under a Creative Commons Attribution NonCommercial License 4.0 (CC BY-NC).